Available online at www.sciencedirect.com
SCIENCE DIRECT®
Journal of Sound and Vibration 272 (2004) 909–936
JOURNAL OF SOUND AND VIBRATION
www.elsevier.com/locate/jsvi

A theoretical study on the influence of the track on train-induced ground vibration

X. Sheng[a,1], C.J.C. Jones[b,*], D.J. Thompson[b]

[a] *Civil Engineering Department, East China Jiaotong University, Nanchang, Jiangxi 330013, People's Republic of China*
[b] *Institute of Sound and Vibration Research, University of Southampton, Southampton SO17 1BJ, UK*

Received 11 December 2001; accepted 9 April 2003

Abstract

An investigation is presented on the nature of train-induced ground vibration propagation. It is based on a theoretical model for the track and a layered ground. Results are given of the responses of the ground and track to a moving harmonic or quasi-static load on the rails. The dispersion characteristics of the propagating modes of vibration in the track and the ground are presented and the excitation of vibration in the ground via the track is discussed in relation to these propagating wavenumbers. An important feature of the coupled system is the coincidence of a propagating wavenumber in the track and the ground that gives rise to the main peak in the vibration spectrum in the frequency range of interest. It has been observed, in some cases, that when the train speed reaches a value close to the speed of propagating waves in the ground, the response to the quasi-static axle loads of the train reaches a peak. The relationship between this critical speed and the wave speeds in the track and ground is considered in order to investigate the effectiveness of controlling this peak response load speed by increasing the bending stiffness of the track/embankment structure or by reducing its mass. It is found that such treatments may, or may not, have a significant effect depending on the ground stiffness and layering. For the multiple quasi-static moving axle loads of a train the loading has strong, closely spaced harmonic components. The effect on the vibration spectrum of the superposition of vibration from multiple axles is shown to lead to the reinforcement or suppression of some frequencies as a function of axle spacing and speed. This is demonstrated with calculated results.

1. Introduction

Increasing interest is being shown in the study of the vibration in the ground produced by trains. The impetus for much of this has been the recognition that in certain circumstances the

*Corresponding author. Tel.: +44-23-8059-3224; fax: +44-23-8059-3190.
E-mail address: cjcj@isvr.soton.ac.uk (C.J.C. Jones).
[1] Currently on leave at ISVR, University of Southampton, England.

0022-460X/$ - see front matter © 2003 Elsevier Ltd. All rights reserved.
doi:10.1016/S0022-460X(03)00781-8

operation of high-speed trains could lead to increased vibration. Two aspects of this are of concern to different groups of engineers. The vibration produced in the ground and propagated away from the track to line-side buildings concerns those evaluating the environmental impact of new lines. In most cases this is dealt with in a similar manner to environmental noise. Track engineers, on the other hand, will be concerned about possible high dynamic displacements in the track structure itself. The concerns in that case include vehicle ride and safety, possible damage to the ballast or embankment materials and the effects of large displacements on very close line-side structures such as electrification masts. Those dealing with environmental vibration may also be concerned with the dynamics of the track, especially where modification to the track structure may be a means of controlling vibration. For example Kaynia et al. [1] have considered using a stiff beam under the track to reduce environmental vibration.

Because of the interest in the field in recent years, a number of models for vibration from trains have been developed [1–5]. Most of these models only take into account the vibration generated by moving, 'quasi-static' axle loads. Ground vibrations induced by these moving axle loads are independent of the dynamics of the vehicles and of track quality. Lai et al. [4] show, by comparison with measurement results, that predictions from such a model may underestimate the actual response level, especially for higher frequencies, as a result of excluding responses to dynamic excitations at wheel–rail contact points.

A model has previously been produced by Sheng et al. [6] for the propagation of vibration from a single oscillating load, moving along a railway track coupled to the ground; the ground is modelled as a layered half-space. In another paper [7], this is extended by coupling, via multiple wheel/rail contact points, to models representing a number of carriages. This model can be used to predict environmental vibration. It includes vibration components from the quasi-static loading of the multiple axles of a moving train and the excitation of dynamic forces due to the undulations of the track top. In the present paper, this track and ground model is used to examine the effects of the coupling between the track structure and the ground. Such an investigation is important for the understanding of the overall mechanisms involved in the generation of ground vibration from trains. The resonance of the track and ground at the cut-on frequency of the ground is examined. It is shown that this can be understood from the dispersion plots of the track and ground. This leads to some conclusions on the phenomenon of the 'critical train speed' which, as it is approached, has been observed to lead to a strong increase in the vibration levels of the track and ground surface (e.g., [8]). Observations are also made concerning the idea of increasing the track/embankment bending stiffness or reducing its mass as a means of avoiding this phenomenon. The harmonic components generated by the passage of the axles of similar wagons are examined by accounting for multiple moving harmonic loads of a single frequency.

2. The model

A diagram of the model of the track and ground system based on Ref. [6] is shown in Fig. 1. A ballasted railway track is aligned in the x direction and has a contact width $2b$ with the ground surface. The mass per unit length and bending stiffness of the two rails taken as a single Euler beam are denoted by m_R and EI, respectively. The lower 'beam', representing the sleeper mass, has a mass m_S per unit length but no bending stiffness. The rail pad is represented by the complex

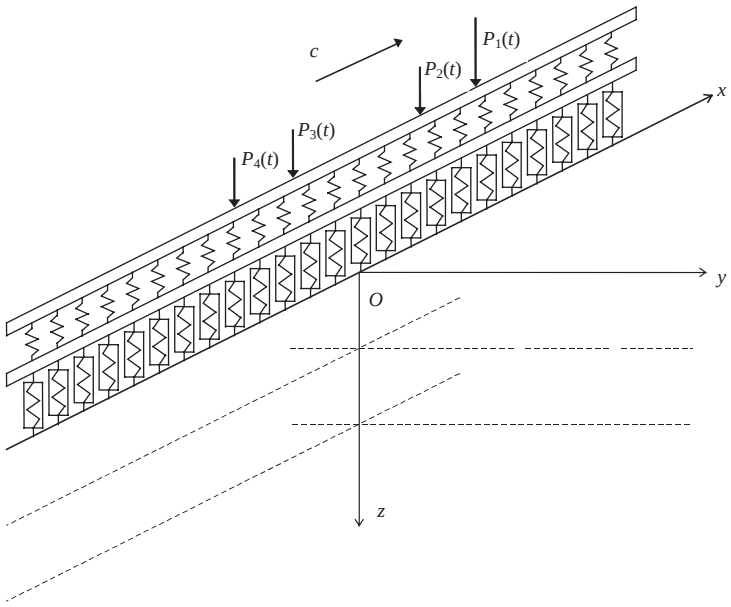

Fig. 1. Model for the track/ground system with multiple moving loads.

stiffness $k_P = k'_p(1 + i\eta_P \operatorname{sgn}(\omega))$ between these two beams, where k'_p is the stiffness of the rail pads for a unit length of track, η_P is the damping loss factor and ω is the circular frequency. The ballast is modelled as a visco-elastic layer with a lateral width $2b$ and an infinite length. Its mass per unit track length is denoted by m_B and only the vertical complex stiffness k_B is taken into account. The loss factor of the ballast is denoted by η_B. Having considered that the sleepers and ballast distribute the vertical wheel–rail forces onto the ground over the width of the track structure, it is assumed that there is only a normal contact force in the contact plane which is uniformly distributed in the y direction from $y = -b$ to b.

The vertical moving forces are denoted by $P_1(t), P_2(t), \ldots, P_M(t)$, from right to left, where M is the number of the forces. At time $t = 0$, the longitudinal co-ordinates of the forces are denoted by $a_1, a_2, \ldots, a_M$. The forces move uniformly along the rail in the positive direction at the train speed c. The vertical displacements of the rail and sleeper are denoted by $w_R(x, t)$ and $w_S(x, t)$. The model calculates the longitudinal, lateral and vertical downwards displacements of any point (x, y) on the ground surface, denoted by $u_{10}(x, y, t)$, $v_{10}(x, y, t)$ and $w_{10}(x, y, t)$. However, only the vertical component is considered in the present study.

The ground is modelled as a layered elastic medium of infinite extent. Within each of the parallel layers the ground is isotropic and homogeneous. In Ref. [6], flexibility matrices are derived for each layer that relate the stresses and displacements at the top of the layer to those at the bottom of the layer. A flexibility matrix is also derived for the half-space substratum. These are combined to form a flexibility matrix representing the response at the surface of the whole ground. These are all functions of the wavenumbers in the x and y directions.

The differential equation of motion of the rail beam is given by

$$EI\frac{\partial^4 w_R(x,t)}{\partial x^4}+m_R\frac{\partial^2 w_R(x,t)}{\partial t^2}+k_P[w_R(x,t)-w_S(x,t)]=\sum_{l=1}^{M}\delta(x-ct-a_l)P_l(t), \tag{1}$$

where $\delta(.)$ is the Dirac-delta function. Eq. (1) is the same as that in Ref. [6] except for the forcing function. The forcing function in the case of multiple forces is

$$P(x,t)=\sum_{l=1}^{M}\delta(x-ct-a_l)P_l(t). \tag{2}$$

It is assumed, in the present paper, that the forces $P_l(t)$ are harmonic with the same circular frequency Ω, i.e.,

$$P_l(t)=\tilde{P}_l(\Omega)\mathrm{e}^{\mathrm{i}\Omega t}\quad (l=1,2,\ldots,M) \tag{3}$$

where $\tilde{P}_l(\Omega)$ is the complex amplitude of the lth force. Thus, Eq. (2) becomes

$$P(x,t)=\sum_{l=1}^{M}\delta(x-ct-a_l)\tilde{P}_l(\Omega)\mathrm{e}^{\mathrm{i}\Omega t}. \tag{4}$$

By applying the single-dimensional Fourier transform pairs

$$\bar{f}(\beta,t)=\int_{-\infty}^{\infty}f(x,t)\mathrm{e}^{-\mathrm{i}\beta x}\,\mathrm{d}x,\quad f(x,t)=\frac{1}{2\pi}\int_{-\infty}^{\infty}\bar{f}(\beta,t)\mathrm{e}^{\mathrm{i}\beta x}\,\mathrm{d}\beta. \tag{5}$$

Eq. (4) yields

$$\bar{P}(\beta,t)=\tilde{P}(\Omega)\mathrm{e}^{\mathrm{i}(\Omega-\beta c)t}, \tag{6}$$

where

$$\tilde{P}(\Omega)=\tilde{P}=\sum_{l=1}^{M}\tilde{P}_l(\Omega)\mathrm{e}^{-\mathrm{i}\beta a_l}. \tag{7}$$

Compared with the case of a single moving harmonic force, Eq. (6) represents a single 'equivalent load' in the wavenumber domain. The amplitude of this equivalent load is given by Eq. (7), and is a function of wavenumber β. Therefore, the approach developed to solve the differential equations of the track–ground system in Ref. [6], can be applied here straightforwardly.

Using the superposition principle, the vertical displacement on the ground surface due to excitation at frequency Ω is given by

$$w_{10}(x,y,t)=\sum_{l=1}^{M}[w_{10}^{\Omega}(x-a_l-ct,y)\tilde{P}_l(\Omega)]\mathrm{e}^{\mathrm{i}\Omega t}, \tag{8}$$

where $w_{10}^{\Omega}(x,y)$ is the displacement amplitude produced by a single unit harmonic load of frequency Ω moving at speed c and observed in the moving frame of reference.

In previous work [6,9], results have been presented as the displacement response in the moving frame of reference due to a single moving load oscillating at a single frequency. These visualizations of the surface wave-field are instructive, but, for the effects of multiple loads, it is

important to derive spectra of vibration response at particular fixed positions. By this means, a presentation of results closer to that obtained by measurements may be achieved.

The vertical displacement spectrum of $w_{10}(x,y,t)$ is denoted by $S_w(x,y,f;\Omega)$, where f is the frequency at which the spectrum is evaluated. Due to motion, a single frequency Ω generates multiple frequencies f. Fourier transforming Eq. (8) with respect to time t, gives the ground surface displacement spectrum expressed in terms of the summation of individual loads, i.e.,

$$S_w(x,y,f;\Omega) = S_w^0(x,y,f;\Omega)\left(\sum_{l=1}^{M}\tilde{P}_l(\Omega)\mathrm{e}^{-\mathrm{i}a_l(\Omega-2\pi f)/c}\right), \tag{9}$$

where $S_w^0(x,y,f;\Omega)$ is the displacement spectrum due to a single unit harmonic force of frequency Ω moving along the rail at speed c. Eq. (9) indicates that the magnitude of spectrum for the multiple moving harmonic forces is independent of the distance x along the track, just as it is for a single load [6].

The term

$$S_P(f) = \sum_{l=1}^{M}\tilde{P}_l(\Omega)\mathrm{e}^{-\mathrm{i}a_l(\Omega-2\pi f)/c} \tag{10}$$

in Eq. (9) may be identified as the load spectrum which reflects the harmonic components of the excitation produced by the passage of the axles of a train. Since a shift of x co-ordinates does not change the magnitude of the load spectrum, the magnitudes of the displacement (velocity or acceleration) spectra are independent of the absolute positions of the multiple, single-frequency, forces.

3. Parameters for track–ground systems

This investigation is performed using numerical results from the above model. The numerical results are presented for two ballasted tracks (one lighter and one heavier) and two grounds (one stiffer and one softer), combinations of which result in four track–ground systems. The parameters of the tracks and the grounds assumed for this study are listed in Tables 1–4. It has been found [10], for the frequency range between about 2 and 100 Hz, that it is usually sufficient to model real soils as a single layer of weathered material about 2 m deep overlying a half-space of stiffer material. The parameters of Table 1 represent a London Clay site in this way and those of Table 2 a site of alluvial soil overlying gravel deposits. The important parameters of interest in the present study are the wave speeds of the materials in each layer.

In order to demonstrate the vibration characteristics of the ground and its response to a load, Section 4.1 presents the dispersion characteristics of the ground and Section 4.2 investigates the surface receptance of the ground as a function of the track wavenumber. Sections 4.3 and 4.4 present the dispersion curves for the grounds and the tracks. Section 4.5 presents the receptances of the tracks and grounds to demonstrate the effect of the resonance of the track and ground at the first cut-on frequency of the layered ground.

Results for the response to moving quasi-static axle loads are investigated in Section 5. Section 5.1 uses results for a single axle load to show the effect of the critical train speed for the

Table 1
Parameters for a stiffer ground

Layer	Depth (m)	Young's modulus (10^6 N/m^2)	Poisson ratio	Density (kg/m^3)	Loss factor	P-wave speed (m/s)	S-wave speed (m/s)	Rayleigh wave speed (m/s)
1	2.0	60	0.44	1500	0.1	360	117.9	112
Half-space		360	0.49	2000	0.1	1755	245	233

Table 2
Parameters for a softer ground

Layer	Depth (m)	Young's modulus (10^6 N/m^2)	Poisson ratio	Density (kg/m^3)	Loss factor	P-wave speed (m/s)	S-wave speed (m/s)	Rayleigh wave speed (m/s)
1	2.0	30	0.47	1550	0.1	340	81.1	77
Half-space		360	0.49	2000	0.1	1755	245	233

Table 3
Parameters for a lighter ballasted railway track

Mass of rail beam per unit length of track	120 kg/m
Bending stiffness of rail beam	1.26×10^7 N m^2
Loss factor of the rail	0.01
Rail pad stiffness	3.5×10^8 N/m^2
Rail pad loss factor	0.15
Mass of sleepers per unit length of track	490 kg/m
Mass of ballast per unit length of track	1200 kg/m
Ballast stiffness per unit length of track	3.15×10^8 N/m^2
Loss factor of ballast	1.0
Contact width of railway and ground	2.7 m

Table 4
Parameters for a heavier ballasted railway track

Mass of rail beam per unit length of track	120 kg/m
Bending stiffness of rail beam	1.26×10^7 N m^2
Loss factor of the rail	0.01
Rail pad stiffness	3.5×10^8 N/m^2
Rail pad loss factor	0.15
Mass of sleepers per unit length of track	490 kg/m
Mass of ballast per unit length of track	3300 kg/m
Ballast stiffness per unit length of track	1.775×10^8 N/m^2
Loss factor of ballast	1.0
Contact width of railway and ground	2.7 m

two tracks and grounds. The speeds that are found are interpreted in terms of the dispersion characteristics of the track and ground combination. Section 5.2 presents results for multiple loads in order to demonstrate the effect of the pattern of the axles of a train.

4. Results for harmonic loading

4.1. The dispersion characteristics of the ground only

Fig. 2 shows the propagating wavenumbers in the softer ground (Table 2) for the P-SV modes plotted against frequency. It is these modes, involving compression and vertical shear motion, not the horizontal shear modes (SH), that are excited by a vertical load (see Appendix A). On this dispersion diagram, the phase velocity of a propagating mode at a particular frequency is given by the inverse slope of a straight line from the origin to the point on its dispersion curve at that frequency. The group velocity, i.e., the speed of transport of energy by the propagating wave, is given by the inverse slope of the dispersion curve itself. The cut-on frequencies of the ground, at which propagating modes in the free ground first appear, can be seen in Fig. 2 to be at 13, 27, 51, 70 and 93 Hz. These modes all cut-on at the wavenumber of the shear wave in the half-space substratum. The P-SV mode dispersion curves for the stiffer ground are given in Fig. 3. In this case propagating modes appear at 22, 47 and 83 Hz. These dispersion diagrams are obtained by an eigenvalue analysis of the ground system equations [6] with the damping set to zero. An explanation of the method of calculation of the dispersion curves from the theory presented in Ref. [6] is given in Appendix A.

An alternative method of identifying the dispersion curves is to calculate the Fourier transformed displacements generated by a load for different frequencies and wavenumbers, and then project the displacement peaks on the wavenumber–frequency plane. As an example, the

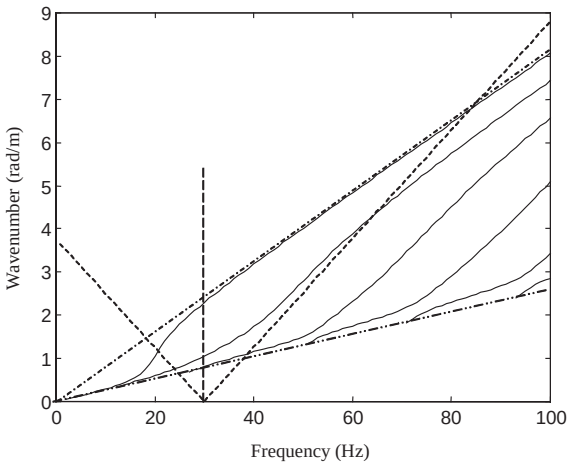

Fig. 2. P-SV dispersion curves of the softer ground (——) and load speed lines (– – –). Load frequency 30 Hz, load speed 0 and 50 m/s. Also plotted are Rayleigh wave of the upper layer (– · –) and shear wave of the underlying half-space (– · · –).

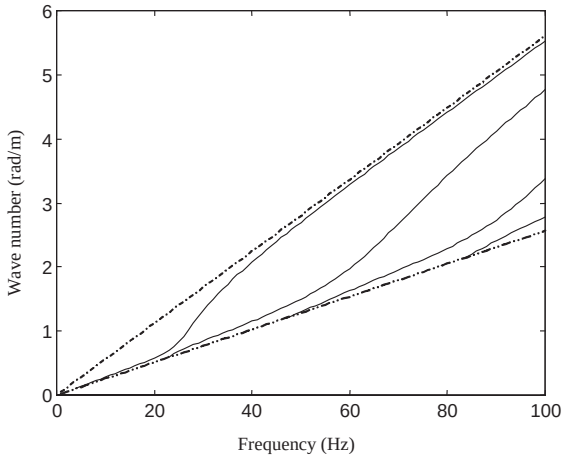

Fig. 3. P-SV dispersion curves of the stiffer ground (——). Also plotted are the Rayleigh wave of the upper layer (– · –) and shear wave of the underlying half-space (– · · –).

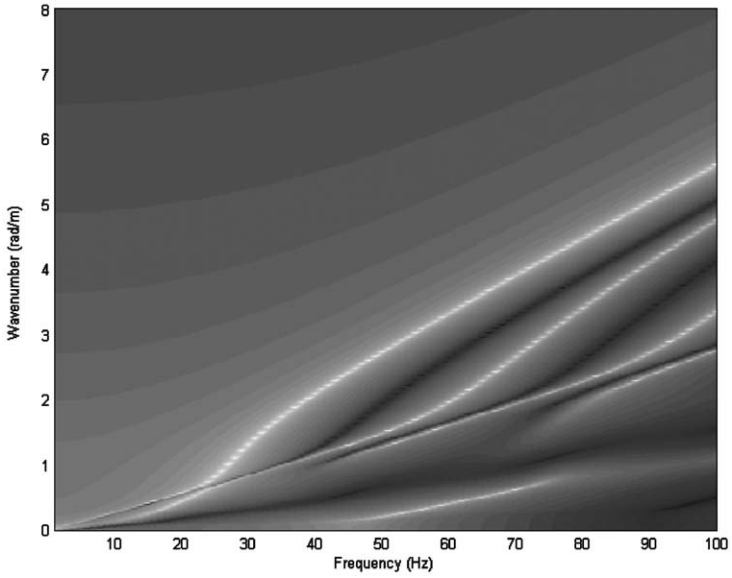

Fig. 4. Shaded representation of the amplitudes of the transformed vertical displacements of the stiffer ground surface (without track) versus wavenumber in the track direction and frequency (light = high amplitude).

amplitudes of the transformed vertical displacements are calculated for the stiffer ground surface generated by a unit vertical point harmonic load. If the amplitudes are plotted three-dimensionally against wave number β in the x direction (the wave number γ in the y direction has been set to zero) and frequency f, then peaks in this plot indicate the propagating wave modes. Such a three-dimensional plot is produced, using shading to represent the height of the peaks, in Fig. 4. The singularities that, in the absence of damping, form the lines of the dispersion

diagram, become peaks in the amplitude of response for the model of the ground that includes damping. Thus the P-SV dispersion curves are revealed in Fig. 4. The figure indicates that, in addition to the propagating wave modes shown in Fig. 3, for some frequencies, an extra mode which has a higher wave speed than the shear wave speed in the underlying half-space is also excited by the surface load (see between 40 and 75 Hz). This extra mode is a so-called 'leaky mode' [11] associated with the interface between the layer and the half-space materials. In Ref. [11] it is shown that these waves radiate energy into the substratum and therefore do not propagate far laterally. Although, as Fig. 4 shows, this mode has an observable amplitude at the surface under the load, it does not normally play an important part in the transmission of vibration across the ground surface.

4.2. The receptance of the ground as a function of wavenumber along the track

It has been shown in Ref. [6] that the coupling of the track with the ground is achieved via the use of the term $\tilde{H}(\beta)$. $\tilde{H}(\beta)$ represents the Fourier transformed (with respect to x only) steady state vertical displacements of points on the x-axis due to a unit vertical harmonic load (moving or stationary) of frequency Ω distributed uniformly in the y direction over the width $|y| \leqslant b$. That is, it is the vertical direct receptance of the ground due to a spatially harmonic load of wavenumber β in the x direction. $\tilde{H}(\beta)$ is given by an infinite integral

$$\tilde{H}(\beta) = \frac{1}{\pi} \int_0^\infty \tilde{Q}_{33}(\beta, \gamma, \Omega - \beta c) \frac{\sin \gamma b}{\gamma b} \, \mathrm{d}\gamma \tag{11}$$

where $\tilde{Q}_{33}$ is the term of the flexibility matrix of the ground giving the vertical response to a vertical load. It is used here as a moving-load Green's function of the ground [6,12].

It can be seen from Eq. (11) that $\tilde{H}(\beta)$ is independent of the railway track parameters except for the width of its contact with the ground surface. The spatial distribution of that load in the x direction is contained in the description $\tilde{H}(\beta)$ since it is expressed as a function of the wavenumber in the track and the distribution as a function of x is recoverable from $\tilde{H}(\beta)$ by the inverse Fourier transform. For now, however, $\tilde{H}(\beta)$ allows the coupling between the track and ground to be examined in terms of the wavenumbers of waves propagating in the ground.

With no damping, an unbounded $\tilde{H}(\beta)$ occurs in response to an excitation at a wavenumber on the dispersion curve. The wavenumbers excited by a moving load are represented by a 'load speed line' defined by $\beta = |\Omega - 2\pi f|/c$. In other words, at the intersections on the dispersion diagram of the dispersion curves and the line $\beta = |\Omega - 2\pi f|/c$ an infinite response appears. When the damping in the ground is considered finite, peaks occur at these values of β. For example Fig. 2 shows load speed lines corresponding to $\Omega/2\pi = 30$ Hz and $c = 0$ and $c = 50$ m/s.

$\tilde{H}(\beta)$ has been calculated for $\Omega/2\pi = 30$ Hz for the softer ground for load speeds $c = 0$ (Fig. 5) and $c = 50$ m/s (Fig. 6). The negative imaginary part of $\tilde{H}(\beta)$ represents the 'active' component that determines the power flow from the load applied by the track into the ground and the real part of $\tilde{H}(\beta)$, the 'reactive' part, i.e., the part of the amplitude of vibration response that does not lead to propagation away into the ground. Fig. 5, for $c = 0$, shows that the highest amplitude peak corresponds to the wavenumber of the first mode at frequency 30 Hz ($\beta \cong 2.4$ radians/m, see Fig. 2). At this wavenumber, the active component is high and the reactive component goes through zero indicating that the amplitude of vibration excited at this wavenumber is associated

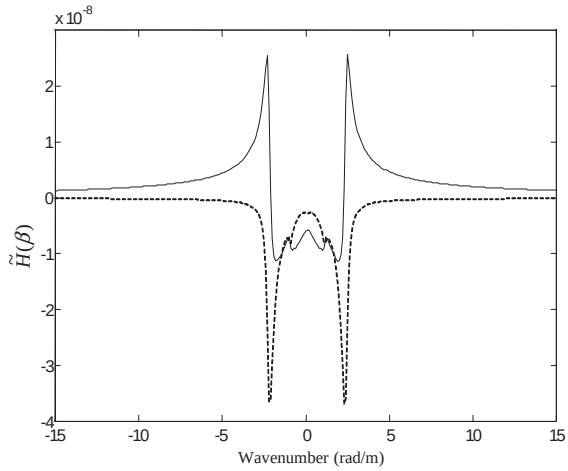

Fig. 5. $\tilde{H}(\beta)$ calculated for the softer ground with $c = 0$, $\Omega/2\pi = 30$ Hz. ——, real part; – – –, imaginary part of $\tilde{H}(\beta)$. When $c = 0$, $\tilde{H}(\beta)$ is an even function of β.

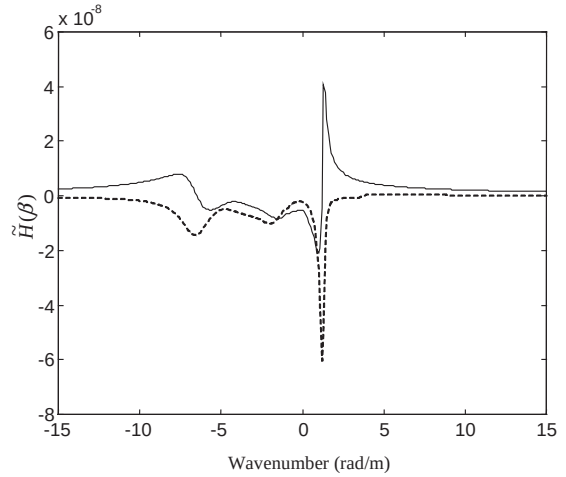

Fig. 6. $\tilde{H}(\beta)$ calculated for the softer ground with $c = 50$ m/s, $\Omega/2\pi = 30$ Hz. ——, real part of $\tilde{H}(\beta)$; – – –, imaginary part of $\tilde{H}(\beta)$.

with a wave propagating away into the ground and that the ground appears to the load as a damper (i.e., carrying away energy). It can be seen that, when $|\beta|$ is larger than this (shorter wavelengths), the imaginary part of $\tilde{H}(\beta)$ decays quickly and the real part is positive. The ground therefore behaves as a spring stiffness and little energy is propagated into the ground. Since the reactive component is the higher of the two at these wavenumbers, these waves are expected to contribute mainly to the near field. At small wavenumbers (large wavelengths) the behaviour is approximately mass-dominated (the receptance has a negative real part).

Fig. 6, for $c = 50$ m/s, shows peaks in the imaginary part at wavenumbers of 1.1 and -6.8 rad/m, corresponding to the intersections of the load speed line and the first wave in Fig. 2. This figure

shows the same behaviour as the stationary load case for the active and reactive components but the two peaks corresponding to the main propagating wave going backwards and forwards are shifted in accordance with the Doppler effect. The peak at 1.1 rad/m has a larger amplitude and that at −6.8 rad/m a smaller amplitude than in the stationary load situation, indicating a greater response in the wave behind the load than in front.

4.3. Dispersion curves of the tracks and the grounds together

As discussed above, the dispersion curves of a free ground (a ground without a track structure) may be calculated by finding the real roots for the dispersion equation. The P-SV dispersion curves of the softer ground have been shown in Fig. 2 while those for the stiffer ground are shown in Fig. 3. However, for a ground with a track, this method is not applicable and the method of identifying the dispersion curves using the shaded plot of the response to discrete frequencies of excitation, as in Fig. 4, has been used.

When a track rests on a ground, the propagation properties of the ground are different in different directions. Since the track is modelled as a two-dimensional structure located in the xz-plane, the propagation property in the y direction is not affected by the presence of the track. However, in the x direction, the propagation property of the ground will be modified by the track. Fig. 7 shows the shaded plot of the amplitudes of the Fourier transformed vertical displacements of the surface of the stiffer ground in the presence of the heavier track. These displacements are produced by a unit stationary harmonic load acting on the rails. Comparing Figs. 4 and 7, it can be seen that, not only the modes of the free ground, but also other modes are excited. These new modes, particularly those with the highest wavenumber, are the propagation modes of the track modifed by its coupling to the ground. Fig. 7 also shows that the first mode of the track–ground

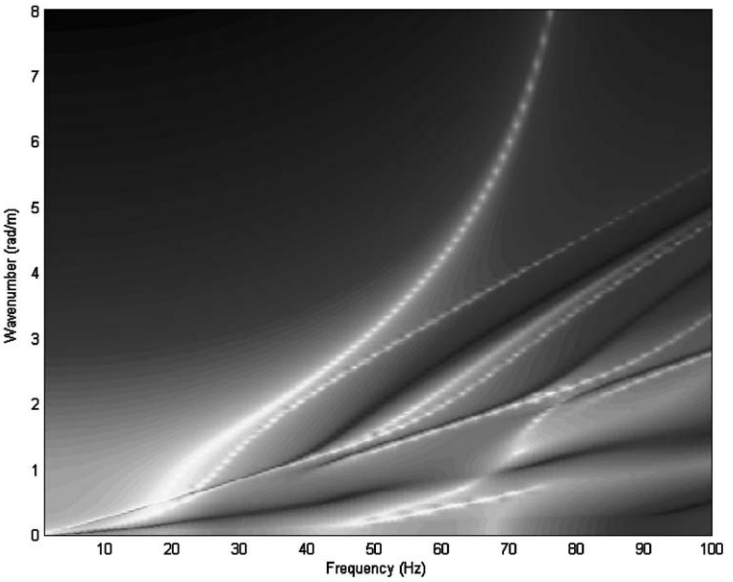

Fig. 7. Shaded representation of the amplitudes of the transformed vertical displacements of the stiffer ground surface with the heavier track versus wavenumber in the track direction and frequency (light = high amplitude).

system has a greater wavenumber, therefore lower phase velocity, than the first mode of the free ground. This mode corresponds to the first mode of the ground carrying the extra mass (and bending stiffness) of the track.

4.4. Dispersion curves for the track only

Eq. (1) is the force balance equation for the rail in the time and spatial domain. Eqs. (40)–(43) of Ref. [13] present the complete force balance equations for the track as a function of the track wavenumber, β, and circular frequency ω. From these equations, the displacement amplitudes of the rail, $\tilde{w}_R$, and the ground surface, $\tilde{w}_{10}$, due to a stationary unit harmonic load can be expressed as

$$\tilde{w}_R(\beta) = \frac{b_1 k_P/\tilde{H}(\beta) + (b_1 a_{22} - b_2 a_{12})}{a_{11} k_P/\tilde{H}(\beta) + (a_{11} a_{22} - a_{12} a_{21})}, \tag{12}$$

$$\tilde{w}_{10}(\beta, \gamma = 0) = \frac{a_{11} b_2 - a_{21} b_1}{a_{11} k_P/\tilde{H}(\beta) + (a_{11} a_{22} - a_{12} a_{21})} \frac{\tilde{Q}_{33}(\beta, 0, \omega)}{\tilde{H}(\beta)}, \tag{13}$$

where $a_{11}, a_{12}, a_{21}, a_{22}, b_1, b_2$ are terms involving the wavenumber, β, frequency, ω, and the mechanical properties of the track. They are:

$$a_{11} = [k_P + k_B - (m_S + \tfrac{1}{3} m_B)\omega^2](EI\beta^4 + k_P - m_R\omega^2) - k_P^2, \tag{14}$$

$$a_{12} = -k_P(k_B + \tfrac{1}{6} m_B \omega^2) \tag{15}$$

$$a_{21} = -(k_B + \tfrac{1}{6} m_B \omega^2)(EI\beta^4 + k_P - m_R\omega^2), \tag{16}$$

$$a_{22} = k_P(k_B - \tfrac{1}{3} m_B \omega^2) \tag{17}$$

$$b_1 = \left[k_P + k_B - (m_S + \tfrac{1}{3} m_B)\omega^2\right], \tag{18}$$

$$b_2 = -(k_B + \tfrac{1}{6} m_B \omega^2). \tag{19}$$

The wavenumbers of the propagating modes of the track–ground system at frequency f may be identified by the fact that, for no damping, both $\tilde{w}_{10}$ and $\tilde{w}_R$ become infinite. Thus, from Eqs. (12) and (13) the dispersion curves of a track on a ground are given by solutions for β of

$$a_{11} k_P/\tilde{H}(\beta) + (a_{11} a_{22} - a_{12} a_{21}) = 0. \tag{20}$$

If $\tilde{H}(\beta)$ is set to infinity, this gives the dispersion equation of a free track (the lower interface of the track structure is unrestrained), i.e.,

$$a_{11} a_{22} - a_{12} a_{21} = 0. \tag{21}$$

If $\tilde{H}(\beta)$ is set to zero, Eq. (20) yields the dispersion equation of a track on a rigid foundation

$$a_{11} = 0. \tag{22}$$

Finally, if $\tilde{H}(\beta)$ is replaced by a constant $1/k_G$, then Eq. (20) results in the dispersion equation of a track on a Winkler foundation, where k_G denotes the complex stiffness of the foundation.

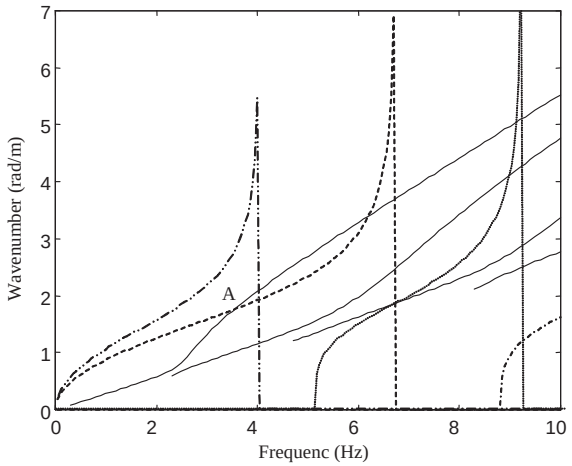

Fig. 8. The dispersion curves of the stiffer ground (——), the free lighter track (– – –), the rigid-bed lighter track (– · –), the free heavier track (– · · –) and the rigid-bed heavier track (···). 'A' indicates intersection of the free lighter track mode curve with the first ground mode curve corresponding to a load speed of 130 m/s.

Compared with the track on a rigid foundation, the presence of the ground adds both flexibility and mass to the track; as a result, the wave speeds in the track are always lower than the wave speeds in the 'rigid-bed track'.

In the absence of a closed-form expression for $\tilde{H}(\beta)$, the analytical formula for the dispersion equation of a track on a ground is not obtainable. As an alternative, the dispersion curves of the free ground, the free track and the rigid-bed track have been produced. Fig. 8 shows these curves for the two tracks and the stiffer ground. From the figure it can be seen that, for a rigid-bed track, a propagating mode exists only at frequencies above the first natural frequency of the track (88 Hz for the lighter track and 51 Hz for the heavy track). For a track with either boundary condition, propagating modes cease to exist at a certain frequency (67 Hz for the lighter free track, 41 Hz for the heavy free track and 92 Hz for the heavier rigid-bed track). This corresponds to the antiresonance of the track in which the mass of sleeper and ballast vibrates on the stiffness of the pad and ballast and the rail does not move. Propagating modes occur again from the second natural frequency of the track.

If at some point (f_0, β_0), the dispersion curve of a free track intersects the dispersion curve of a free ground, then since $\tilde{H}(\beta_0) = \infty$ in the absence of damping (see Section 4.2), Eq. (21) holds at this point. In other words, as a wave can propagate in both the free track and the free ground at speed $2\pi f_0/\beta_0$, this will also be a permissible solution for a propagating wave in the coupled system.

A general analysis is difficult for the existence of propagating modes in a track–ground system (i.e., the existence of real roots of β in Eq. (20)). However, for a track resting on a homogeneous half-space, some points may be made.

For the homogeneous half-space, there is only one straight line on its dispersion diagram, i.e., the Rayleigh wave line. If, for a given frequency, the Rayleigh wave line is below the dispersion curve of the free track but above the dispersion curve of the rigid-bed track, then it can be shown that Eq. (20) has a real solution β, which is greater than the Rayleigh wavenumber but less than

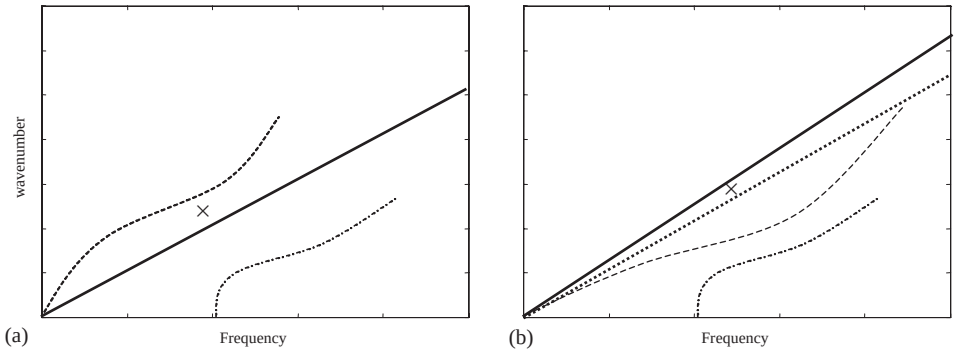

Fig. 9. Diagram showing the relative locations of the dispersion curves of the free track, the fixed-bed track and the ground. (a) When the free track mode has a lower wave speed than the Rayleigh wave in the ground; (b) when the free track mode has a higher wave speed than the Rayleigh wave ——, Rayleigh wave of the ground, ..., shear wave of the ground; – – –, free track mode; – · –, fixed-bed track; ×, position of possible solution.

the wavenumber of the free track. This situation is shown diagrammatically in Fig. 9(a). Alternatively, if the Rayleigh wavenumber is greater than the wavenumber of the free track (therefore it is definitely greater than the wavenumber of the rigid-bed track), as shown in Fig. 9(b), then it can be shown that the only possible real solution to Eq. (20) is a value of β greater than the shear wavenumber but less than the Rayleigh wavenumber in the ground.

In terms of wave speed, therefore, it may be concluded that the phase speed of the lowest order wave in a track resting on a homogeneous half-space cannot exceed the shear wave speed in the half-space. For a light, stiff track it may still exceed the Rayleigh wave speed. For a heavy track the wave speed in the track may be lower than both the shear wave speed and the Rayleigh wave speed.

4.5. *Receptances of the track–ground systems*

4.5.1. *Receptances of the tracks*

Figs. 10 and 11 show the magnitude and phase of the receptances at the loading point on the rails for each track on the softer and stiffer grounds. Also shown are results for the tracks resting on a rigid foundation. It can be seen that, for the two cases that include the ground, there is a peak response around the first ground cut-on frequency. Only at higher frequencies is the difference between the receptances for a ground and a rigid foundation small. The effective stiffness of the track below 10 Hz is characterized by that of the ground and is considerably lower than the stiffness at frequencies well above this first cut-on frequency.

There is a notable likeness in the shape of the spectrum of the predicted track receptances that include the ground and measurements on real track such as those presented by Oscarsson and Dahlberg [14]. Both the amplitude and phase have the same character even though the measurements in Ref. [14] are clearly for a stiffer ground than either of the cases presented here.

4.5.2. *Receptances of the grounds*

Figs. 12 and 13 show the vertical displacements of the ground surface due to a unit stationary harmonic load of varying frequency acting on the rails for the four combinations of the two tracks

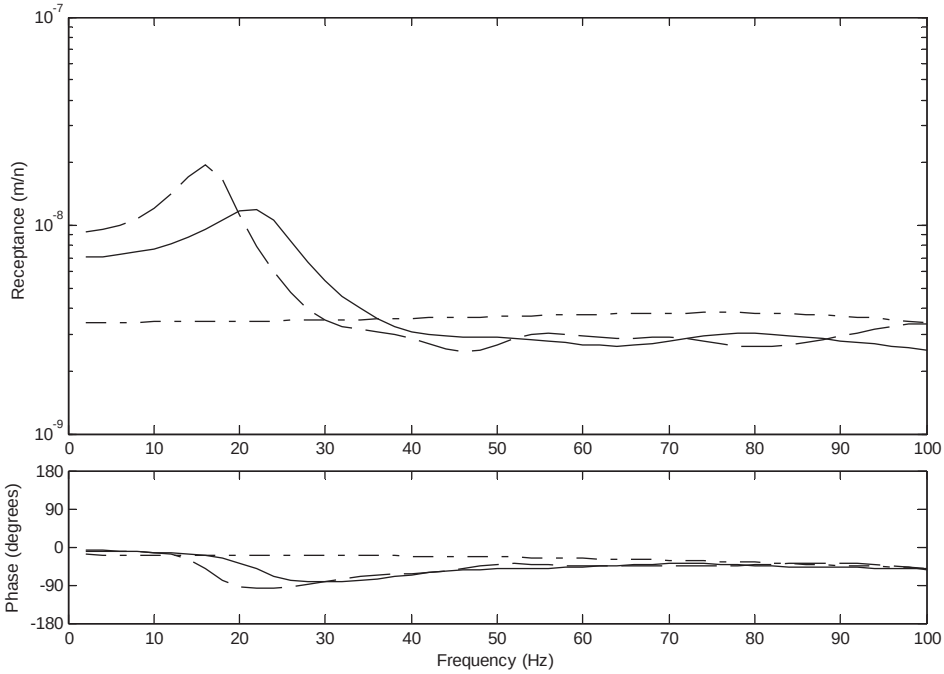

Fig. 10. Receptances (magnitudes and phases) at the loading point on the rail of the lighter track for a stationary load. ——, the track on the stiffer ground; – – –, the track on the softer ground; – – – –, the track on a rigid foundation.

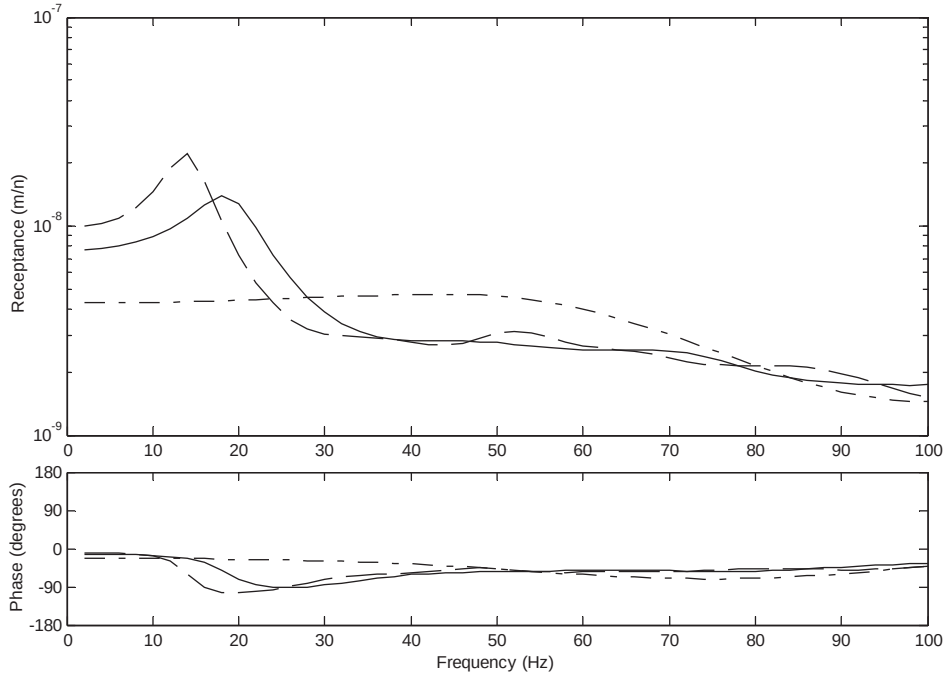

Fig. 11. Receptances (magnitudes and phases) of the loading point on the rail of the heavier track for a stationary load. ——, the track on the stiffer ground; – – –, the track on the softer ground; – – – –, the track on a rigid foundation.

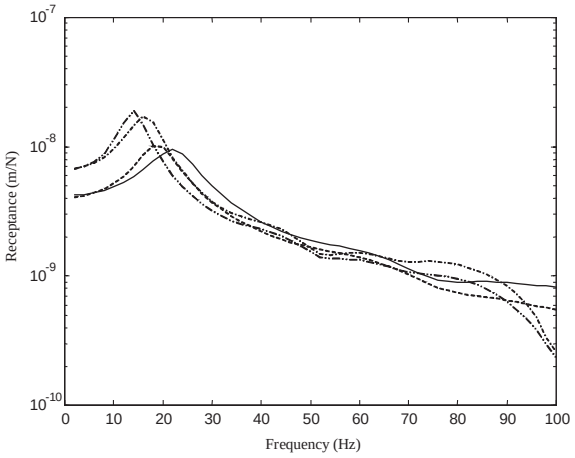

Fig. 12. Receptances (response of the ground to a force on the rail) at $y = 0$ m for a stationary load. ——, lighter track–stiffer ground system; – – –, heavier track–stiffer ground system; – · – · –, lighter track–softer ground system; – · · –, heavier track–softer ground system.

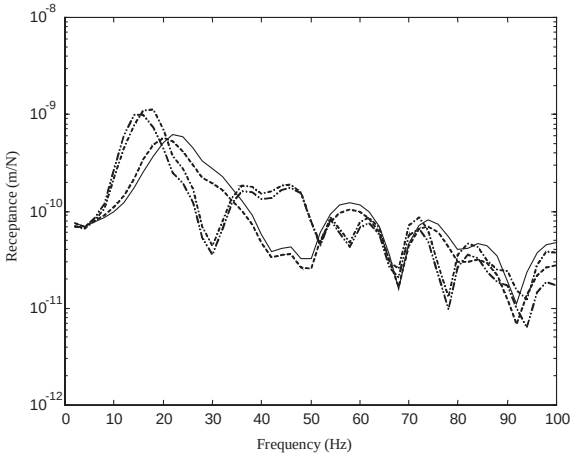

Fig. 13. Receptances (response of the ground to a force on the rail) at $y = 10$ m for a stationary load. ——, lighter track–stiffer ground system; – – –, heavier track–stiffer ground system; – · – · –, lighter track–softer ground system; – · · –, heavier track–softer ground system.

and the two layered grounds. Fig. 12 is for the displacements of the point underneath the load while Fig. 13 is for a point 10 m from the track centreline. It can be seen from Fig. 12 that a resonance occurs when a track rests on a layered ground. The resonance frequency is modified by the presence of the track. For the stiffer ground with the lighter track, the resonance frequency is 22 Hz, identical to the first cut-on frequency of the ground (Fig. 3). However, when the heavier track is present, the resonance frequency is reduced to 18 Hz. In the case of the softer ground, the lighter track increases the resonance frequency from its first cut-on frequency, 13 Hz (Fig. 2), to 16 Hz. With the heavier track the response frequency is almost unchanged, i.e., about 13 Hz.

It is also seen in Figs. 12 and 13 that, at very low frequencies (below 5 Hz), a change in the track mass does not significantly affect the responses of the ground surface. With increasing frequency, the lighter track produces lower responses than the heavier track due to the increase in the resonance frequency. However, for frequencies higher than the resonance frequencies, the heavier track produces less response than the lighter track.

In the transfer receptance to 10 m, Fig. 13, the first trough for the stiffer ground is found at 40 Hz while for the softer ground it is at 30 Hz. The low responses at these frequencies are due to the loading width in the track/ground contact plane, which filters the propagating wave of the first mode at a wavelength identical to the loading width. The contact width of the track/ground is $2b = 2.7$ m (Table 3), which corresponds to a wavenumber of $2\pi/2b = 2.327$ rad/m. In the dispersion diagrams, Fig. 3 for the stiffer ground and Fig. 2 for the softer ground, it can be identified that the frequency corresponding to this wavenumber of the first propagating mode is 40 Hz for the stiffer ground and 30 Hz for the softer ground.

5. Results for quasi-static loading

5.1. Effects of the speed of a single axle load on the responses of track–ground systems

The effects of the speed of a single quasi-static axle load on the responses of track–ground systems are investigated in this section. First in Section 5.1.1, the case of a track resting on a homogeneous half-space is investigated. The situation of a track resting on a layered ground is dealt with in Section 5.1.2.

5.1.1. Track on a homogeneous half-space

Two homogeneous half-spaces, one made of the upper layer material of the stiffer ground (see Table 1), the other made of the upper layer material of the softer ground (see Table 2), are considered here. The maximum displacements along the x-axis on the ground surface due to a single unit constant force have been computed for different speeds and are plotted in Fig. 14. Results are shown for the lighter and heavier tracks on the two homogeneous half-spaces. This figure demonstrates that a sharp increase in vibration occurs as the load speed approaches a certain 'critical' value. The speed at which these curves have their maximum value will be referred to here as the 'peak response load speed'. For the stiffer homogeneous half-space with the lighter track, the peak occurs at a load speed of 112 m/s, which is equal to the Rayleigh wave speed of the ground. For the stiffer homogeneous half-space with the heavier track, the peak appears at 105 m/s, i.e., lower than the Rayleigh wave speed. For the softer homogeneous half-space, the corresponding peaks for both the tracks appear at 77 m/s, the Rayleigh wave speed.

Fig. 15 shows the dispersion curves of the free tracks and the homogeneous half-spaces. Comparison of Figs. 14 and 15 show that, for a track/homogeneous half-space system, if the propagating wavenumber in the free track is greater than the Rayleigh wavenumber at all frequencies, then the peak response load speed is lower than the Rayleigh wave speed. However, if the propagating wavenumber in the free track is equal to the Rayleigh wavenumber at some frequency, then the peak response load speed equals the Rayleigh wave speed, and decreasing the mass of the track further does not increase the peak response load speed.

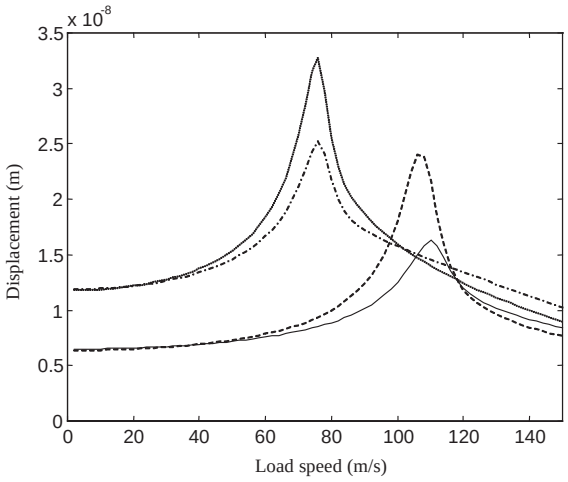

Fig. 14. Maximum displacements along the x-axis on ground surface. ——, the lighter track resting on a half-space of the upper layer material of the stiffer ground; – – –, the heavier track resting on the same half-space; – · –, the lighter track resting on a half-space of the upper layer material of the softer ground; ⋯, the heavier track resting on the same half-space.

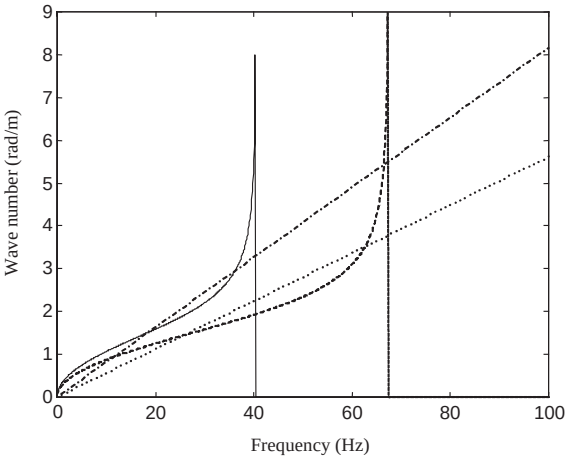

Fig. 15. Dispersion curves of the free tracks and the homogeneous half-spaces. ——, for the heavier track; – – –, for the lighter track; – · –, for the softer homogeneous half-space; ⋯, for the stiffer homogeneous half-space.

Under the action of the moving load, the response of the track/ground contains a broad range of frequency components. This is indicated in Fig. 16, which shows the spectra of vertical velocity responses on the surface of the softer homogeneous half-space due to a unit load moving along the heavier track at the peak response load speed of 77 m/s. The responses are shown at two positions, $y = 0$ and 10 m. A broad peak occurs at a frequency (about 13 Hz) lower than that corresponding to the intersection of the free-track dispersion curve and the Rayleigh wave line of the half-space.

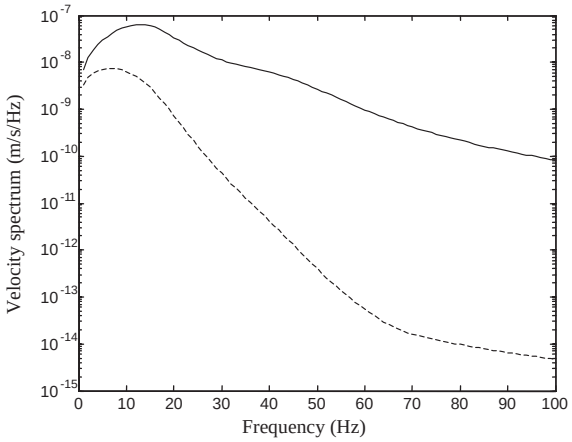

Fig. 16. Magnitudes of the vertical velocity spectra at $y = 0$ m (—) and at 10 m (– – –) on the ground surface for the heavier track on the softer homogeneous half-space when a unit load travels at the peak response load speed (77 m/s).

The shift in peak frequency is due to the material and radiation damping in the track/ground structure.

5.1.2. Track on a layered ground

When a track rests on a layered ground, since there are several propagating modes existing in the system, the effect of the load speed on the response becomes more complicated to analyze.

Fig. 17 shows the maximum displacements of different track and layered ground combinations (corresponding to Tables 1–4) due to a unit constant load moving at different speeds. For the stiffer ground with the lighter track, the peak response load speed is 130 m/s, greater than the Rayleigh wave speed of the upper layer (112 m/s). This speed corresponds to a line passing through the point A in Fig. 8 at which the free track and free-ground dispersion curves intersect. This intersection, it will be recalled, corresponds to a point at which free waves can occur in the coupled track–ground system. The direct excitation of the first mode in the ground and the free track by a constant load travelling at 130 m/s explains the peak response at this speed seen in Fig. 17.

For the heavy track on the stiffer ground, the peak occurs at 110 m/s, a little less than the Rayleigh wave speed of the upper layer of the ground. From Fig. 8, the dispersion curve of the free track is seen to have no intersection with the first dispersion curve of the ground in this case. As in the case of the homogeneous half-space, where the dispersion curves do not intersect, the peak response load speed is below the wave speeds in the ground.

In the case of the softer ground, although not shown graphically here, a similar correspondence has been observed between the peak response load speed and the dispersion curves of the track/ground structure. For the softer ground with the lighter track, the peak response load speed is 105 m/s, greater than the Rayleigh wave speed of the upper layer (77 m/s). For the heavier track resting on the softer ground, the peak load speed is 90 m/s, still greater than the Rayleigh wave speed of the upper layer material, because, in this case, unlike the stiffer ground, the free-track dispersion curve for the heavier track does intersect the curve for the first mode of the free ground.

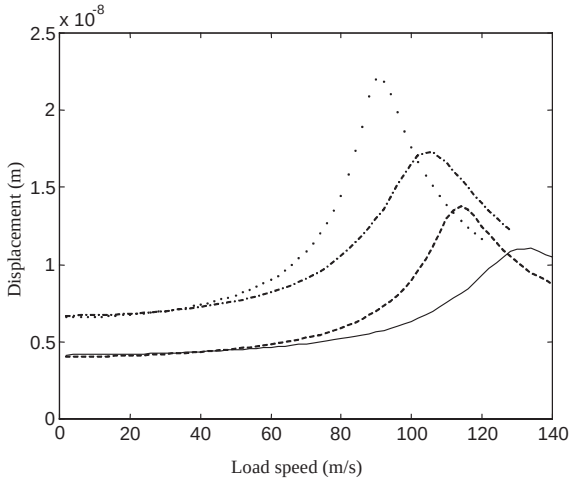

Fig. 17. Maximum displacements along the x-axis on the ground. ——, the lighter track resting on the stiffer ground; – – –, the heavier track resting on the stiffer ground; – · –, the lighter track resting on the softer ground; ⋯, the heavier track resting on the softer ground.

The observations above show that, when a track rests on a layered ground, the peak response load speed may be determined by the first intersection of the free track dispersion curve and the ground dispersion curve of the first mode for all frequencies. In other words, the peak response load speed for a constant load is given by $c = 2\pi f_0/\beta_0$, with β_0 and f_0 denoting the wavenumber and frequency at the intersection. If there is no such intersection, because the free track wave speed is lower than that of the first mode in the ground, then the peak response load speed is lower than the Rayleigh wave speed in the upper layer. The frequency f_0 is found to be 34 Hz for the combination of the lighter track and stiffer ground, 21 Hz for the lighter track on the softer ground, 25 Hz for the heavier track on the softer ground and for the heavier track and softer ground there is no intersection.

The vertical velocity response spectra at $y = 0$ m on the ground surface are shown in Fig. 18 for the four track/ground combinations. In each case, a unit load moves along the track at the peak response load speed for that combination of track and ground. It can be seen that a peak occurs in the spectrum at a frequency lower than the corresponding value of f_0. At very low frequencies, the response at the peak response load speed is not affected by the change in the track mass although the speeds themselves are quite different. Just below the main spectrum peak, the heavier track leads to a higher response than the lighter track but at frequencies much higher than the peak, it leads to lower response. Thus in considering track modification to control the level of vibration *at the peak response speed*, a lighter, stiffer track may not be beneficial at all relevant frequencies, although it must be remembered that the primary effects are those connected to the change of the peak response load speed.

It can be seen in Figs. 14 and 17 that, when the load speed is well below the peak response load speeds, the track mass makes little difference to the ground response; that is the responses for a given ground are independent of the track. However, the peak response amplitude of the ground with the lighter track is much lower than that of the ground with the heavier track. The track mass

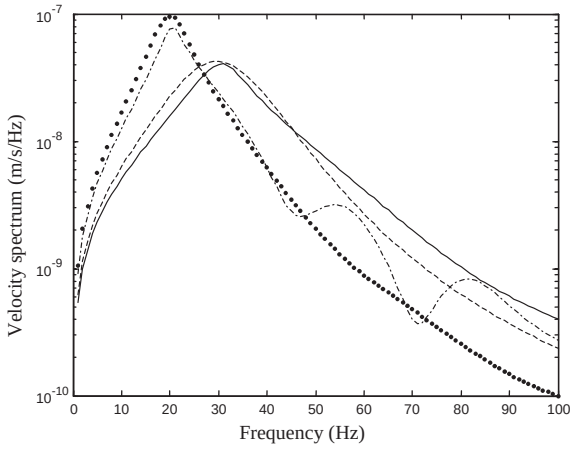

Fig. 18. Magnitude of the vertical velocity spectrum at $y = 0$ m on the ground surface for the four track/ground combinations when a unit load travels at the corresponding peak response load speed. —, the lighter track on the stiffer ground; – – –, the heavier track on the stiffer ground; – · –, the lighter track on the softer ground; ⋯, the heavier track on the softer ground.

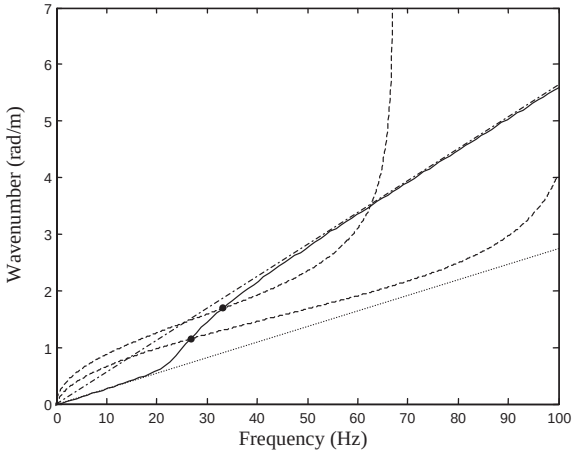

Fig. 19. Diagram showing the change in the peak response load speed due to the shift in the intersection between the free track mode dispersion curve and the ground mode curve when the track mass or stiffness is changed. —, the first mode in a layered ground; – – –, the free track mode; – · –, Rayleigh wave in the upper layer; ⋯, Rayleigh wave in the underlying half-space.

also has a significant effect on the peak response load speed, especially for the layered ground. This can be understood by reference to the dispersion curve of the first mode of the ground and that for the free track. This is illustrated in Fig. 19. Because of the ground mode's transition from being close to the Rayleigh wave speed in the half-space at low frequency to being close to the Rayleigh wave speed of the upper layer at high frequency, its intersection with the free track curve can move relatively rapidly with increasing track stiffness (or decreasing mass). However, this

effect whereby the track mass or stiffness may have a large effect on the peak response load speed depends on the free track curve intersecting the ground mode curve in such a transition where it has a high slope. In cases where the ground behaves like a half-space or the free track curve does not intersect the ground mode curve, the effect of the track on the peak response load speed will be small. If the track mass or stiffness were to be used in practice to control the peak response load speed, such a measure would have to be planned in the light of the knowledge of the dispersion curves of the track and the ground at the particular site.

5.2. Effects of multiple axle loads

This section investigates the effects of multiple axle loads on the responses of track–ground systems. The discussion is based on Eqs. (8) and (9). From Eq. (8), if the loads are axle loads at $\Omega = 0$, the vertical displacement of the ground surface is given by

$$w_{10}(x, y, t) = \sum_{l=1}^{M} w_{10}^{0}(x - a_l - ct, y)\tilde{P}_l, \tag{23}$$

where $\tilde{P}_l$ denotes the magnitude of the lth axle load, $w_{10}(x, y, t)$ the ground surface vertical displacement and $w_{10}^{0}(x, y)$ represents the vertical displacement on the ground surface generated by a single unit constant force moving at speed c. When the load speed is well below the lowest phase speed in the track–ground system, the displacement produced by a single force is attenuated quickly with distance (evanescent wave) and confined near the position of the force. In this case, the maximum displacement produced by the multiple axle loads is not very different from that produced by each single axle load. The situation may be different when the load speed is high enough to excite the propagating wave mode of the track–ground system. In this case, if the distances between adjacent axles are almost the same and close to the wavelength of the propagating mode, then as may be deduced from Eq. (23), the responses produced by each axle load are 'in phase' with each other, and add together to give a higher total response.

However, whatever the train speed is, during the passage of a train of many similar wagons, the pattern of axles of the wagons may give rise to strong harmonic components. Eq. (9) shows that the spectra produced by multiple forces of a single frequency (for the quasi-static loads, this frequency equals zero) are equal to those produced by a unit force of the same frequency moving at the same speed, times the load spectrum. The load spectrum is given by Eq. (10). The spectra vanish at frequencies satisfying $\sum_{l=1}^{M} \tilde{P}_l(\Omega)\mathrm{e}^{-\mathrm{i}a_l(\Omega - 2\pi f)/c} = 0$. In principle, this equation shows that certain frequencies can be eliminated from the excitation of ground vibration by a careful choice of wagon axle spacing. However, this is not likely to be a practical proposition in order to treat problem frequencies that are dependent on the ground and track properties of a particular site. It may, however, offer a choice of speed particular to the vehicle type which reduces certain (narrow) ranges of excitation frequency.

To represent a train consisting of similar two-axle wagons, let $\tilde{P}_l = P$, $l = 1, 2, \ldots, M$, $a_1 = 0$, $a_2 = -b$, $a_3 = -a$, $a_4 = -a - b$, $a_5 = -2a$, $a_6 = -2a - b$, etc., where a is the length of each

wagon, and b the distance between two axles within a wagon. Thus, Eq. (10) becomes

$$S_P(f) = \sum_{l=1}^{M} P e^{i2\pi f a_i/c} = P\sum_{k=1}^{N} e^{-i2\pi f(k-1)a/c} + P\sum_{k=1}^{N} e^{-i2\pi f[(k-1)a+b]/c}$$
$$= P(1 + e^{-i2\pi fb/c})\sum_{k=1}^{N} e^{-i2\pi f(k-1)a/c}, \quad (24)$$

where N denotes the number of wagons. Eq. (24) shows that, at frequencies $f = c/(2b)$ and $f = c/(2a)$ (if N is even) the load spectrum vanishes, while at frequency $f = c/a$, the magnitude of the load spectrum is proportional to the number of wagons. Particularly, when $a = 2b$, i.e., the distance between two adjacent axles either within a wagon or in two adjacent wagons is identical, then at the passing frequency of axles, $f = c/b$, the load spectrum is $2NP$.

To illustrate the harmonic structure of the loading due to multiple axles, the vertical velocity spectra are presented below for six quasi-static loads ($M = 6$), of three two-axle wagons ($N = 3$) [15], which move on the lighter track on the softer ground. The axle spacing b is 8.96 m and the length of a wagon, a, is 13.82 m. The magnitude of force at each axle is set to unity.

Fig. 20 shows the vertical velocity spectra of the ground surface at various distances produced by the six loads moving at $c = 40$ m/s, well below the lowest wave speed of the ground. The vertical velocity spectra produced by a single unit constant force of the same speed are shown in Fig. 21. The load spectrum of the six axle loads, defined by Eq. (10), is shown in Fig. 22. The harmonic nature of the excitation introduced by the multiple axles is clearly indicated by comparing the three figures. Fig. 20 also shows that, for each harmonic component, the attenuation rate near the track is higher than that further away.

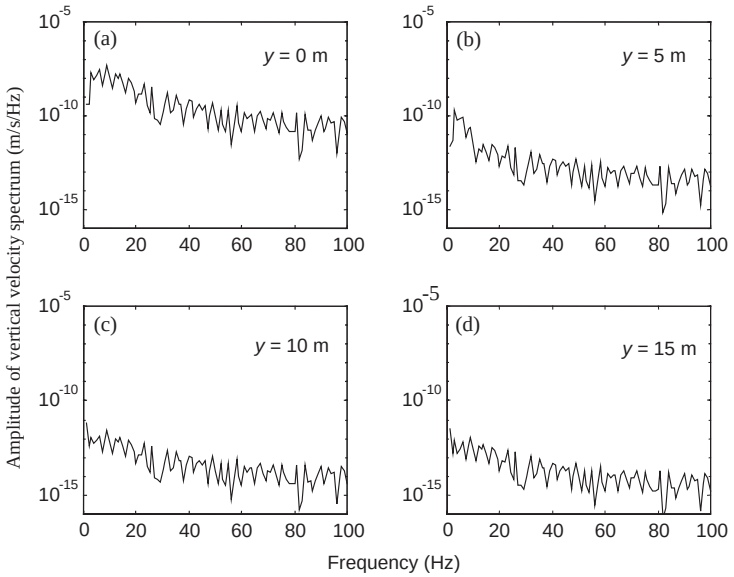

Fig. 20. Vertical velocity spectra of points on the ground surface produced by the six loads moving at 40 m/s. (a) On the track centreline; (b) at 5 m; (c) at 10 m; (d) at 15 m.

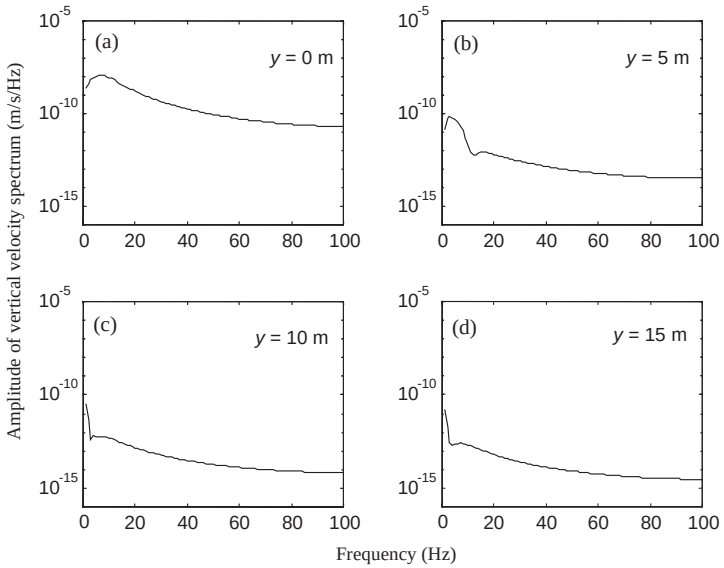

Fig. 21. Vertical velocity spectra of points on the ground surface produced by a single unit constant force moving at 40 m/s. (a) On the track centreline; (b) at 5 m; (c) at 10 m; (d) at 15 m.

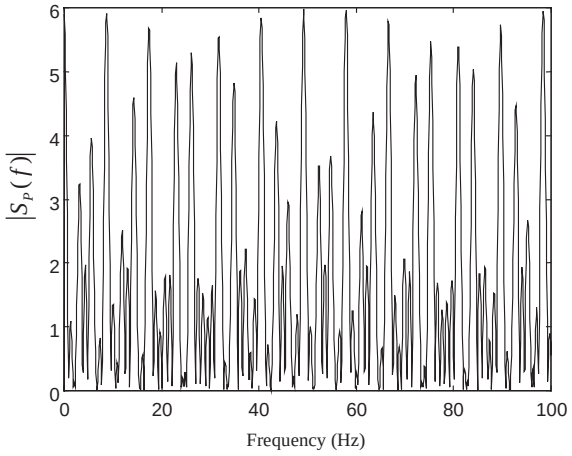

Fig. 22. The 'load spectrum' of the six unit axle loads moving at 40 m/s.

6. Conclusions

In this paper, an investigation has been presented into the nature of ground vibration propagation in a track–ground system using a previously developed model. The concepts of free track, 'fixed-bed' track and free ground are defined and used to develop understanding of the nature of wave excitation and propagation in the track–ground system and, in particular, the phenomenon of a 'critical' speed at which high levels of vibration are induced.

From the example results presented here, several conclusions can be drawn on the response spectrum at the ground to dynamic loading. For a track on a layered ground, near the first cut-on frequency of the free ground, both the track and the ground have maximum (resonance) responses. The presence of a track may increase or decrease the resonance frequency depending on the combination of the ground and the track parameters. The existence of a resonance frequency indicates the layered structure of the ground.

At very low frequencies, change of the track mass does not significantly affect the responses of the ground surface to a unit amplitude force at the track. With increasing frequency, a lighter track produces lower responses than a heavier track due to its higher resonance frequency. However, for frequencies higher than the resonance frequencies, a heavier track produces less response than a lighter track.

The ground may have a great effect on the track response compared with the response of the same track on a rigid foundation, especially for frequencies near the cut-on frequency of the ground. For the dynamics of a track at low frequencies, consideration of the elasticity and energy radiation of the supporting ground is necessary.

The response to a non-oscillating but moving load, has been investigated in terms of the effects of the ground stiffness and track properties on the peak response load speed. For a track on a homogeneous half-space, the peak response load speed of an axle load will not be greater than the Rayleigh wave speed in the half-space. In the dispersion diagram, if the dispersion curve of the free track is above the Rayleigh wave line of the ground, then the peak response load speed is lower than the Rayleigh wave speed. If the dispersion curve of the free track intersects the Rayleigh wave line, then the peak response load speed is equal to the Rayleigh wave speed. Further increasing the track bending stiffness, or decreasing the track mass, does not increase the peak response load speed. Modification to the track mass leads to only a small reduction of vibration when the load speed is well below the peak response load speed. However, when the load speed approaches the peak response load speed, decreasing the track mass has a much greater effect in reducing the level of vibration.

For a track on a layered ground consisting of a single layer on a deep, stiffer substratum which is modelled as a homogeneous half-space, the peak response load speed may be greater than the Rayleigh wave speed associated with the material in the upper layer. The peak response load speed may be determined by the first intersection of the dispersion curve of the free track and that of the first mode of the ground, i.e., given by $2\pi f_0/\beta_0$, where β_0 and f_0 are the wavenumber and frequency at this intersection. Since, for low frequency, the dispersion curve of the first mode of the ground is close to the Rayleigh wave line of the underlying half-space, increasing the track bending stiffness or decreasing the track mass can increase the peak response load speed for the track–ground system so that the peak response load speed is much higher than the Rayleigh wave speed in the upper layer.

During the passage of a train of many similar wagons, the pattern of axles of the wagons may give rise to, or suppress, some harmonic components. These harmonic components are formulated in terms of the dimensions of the wagons as well as of the train speed.

It is worth noting, in addition to the points above, that, for the layered ground, all the main features of the train/track/ground interaction for both harmonic and moving axle-load excitation have been explained in terms of the dispersion characteristics and excitation of the first propagating mode of the ground, rather than any of the higher order modes. Since the first

ground mode dominates both the interaction behaviour and the response, it may be concluded that a method to characterize the ground at a particular site should focus on determining its dispersion characteristic.

Having developed a model to investigate the vibration behaviour of the train/track ground system, work has also recently been carried out to extend this model to provide predictions of vibration spectra from trains. This is reported in Ref. [7]. Comparison of such predictions for three diverse cases where measurement data is available is made in Ref. [16].

Appendix A. Dispersion curves of a layered ground

An undamped ground can sustain free propagating waves in which each particle of the ground vibrates harmonically at a single frequency. The wavenumbers of the free propagating waves depend on the frequency of vibration. These free propagating waves are termed *the propagating modes* (or simply *the modes*) *of the ground*. The propagating modes may be divided into two types: the P-SV modes (waves) and the SH modes (waves). For a P-SV mode, particles in the ground have displacement components not only in the vertical direction but also in the horizontal propagation direction while for a SH mode, the particles vibrate only in a direction parallel to the ground surface but perpendicular to the horizontal propagation direction. The P-SV modes and the SH modes in the ground can be uncoupled.

The dispersion curves, which are defined as wavenumbers of propagating modes (P-SV and SH modes) in the ground plotted against frequency, are helpful in the investigation of the mechanism of ground vibration, as seen in this paper. There are different methods to calculate the dispersion curves [12]. The formulae developed in Ref. [6] may also be applied to produce the dispersion curves. From Eqs. (27) and (28) in Ref. [6], the Fourier transformed displacements and loads (pressures) on the ground surface are related by

$$([\mathbf{T}]_{21} - [\mathbf{S}][\mathbf{R}]^{-1}[\mathbf{T}]_{11})\{\tilde{\mathbf{u}}\}_{10} = ([\mathbf{T}]_{22} - [\mathbf{S}][\mathbf{R}]^{-1}[\mathbf{T}]_{12})\{\tilde{\mathbf{p}}\}, \tag{A.1}$$

where $\{\tilde{\mathbf{u}}\}_{10}$ and $\{\tilde{\mathbf{p}}\}$ are the Fourier transformed displacement vector and the Fourier transformed load vector on the ground surface, $[\mathbf{R}]$ and $[\mathbf{S}]$ are (3×3) matrices determined by the property of the underlying half-space, and $[\mathbf{T}]_{11}$, etc. are (3×3) matrices concerning the soil layers. Putting $\{\tilde{\mathbf{p}}\} = 0$ in Eq. (A.1) results in the so-called free vibration equation of the ground

$$([\mathbf{T}]_{21} - [\mathbf{S}][\mathbf{R}]^{-1}[\mathbf{T}]_{11})\{\tilde{\mathbf{u}}\}_{10} = 0. \tag{A.2}$$

For non-zero solutions to exist, the determinant of the coefficient matrix of Eq. (A.2) must be equal to zero, i.e.,

$$\det([\mathbf{T}]_{21} - [\mathbf{S}][\mathbf{R}]^{-1}[\mathbf{T}]_{11}) = 0. \tag{A.3}$$

For a given frequency f, the real values of β, γ satisfying Eq. (A.3), give the wave numbers of propagating wave modes at that frequency (the waves propagating in the x and y directions). Eq. (A.3) is termed the dispersion equation of the ground.

Denoting the matrix $[\mathbf{T}]_{21} - [\mathbf{S}][\mathbf{R}]^{-1}[\mathbf{T}]_{11}$ by $[\mathbf{D}(\beta, \gamma, \omega)]$ and $[\mathbf{T}]_{22} - [\mathbf{S}][\mathbf{R}]^{-1}[\mathbf{T}]_{12}$ by $[\mathbf{D}'(\beta, \gamma, \omega)]$, it can be shown that

$$[\mathbf{D}(\beta, \gamma, \omega] = [\mathbf{A}][\mathbf{D}(0, \rho, \omega)][\mathbf{A}]^{\mathrm{T}}, \tag{A.4}$$

$$[\mathbf{D}'(\beta,\gamma,\omega] = [\mathbf{A}][\mathbf{D}'(0,\rho,\omega)][\mathbf{A}]^{\mathrm{T}}, \tag{A.5}$$

where

$$[\mathbf{A}] = \begin{bmatrix} \sin\phi & \cos\phi & 0 \\ -\cos\phi & \sin\phi & 0 \\ 0 & 0 & 1 \end{bmatrix}, \quad \rho = \sqrt{\beta^2+\gamma^2}, \quad \cos\phi = \beta/\rho, \quad \sin\phi = \gamma/\rho, \tag{A.6}$$

$$[\mathbf{D}(0,\rho,\omega)] = \begin{bmatrix} d_{11} & 0 & 0 \\ 0 & d_{22} & d_{23} \\ 0 & d_{32} & d_{33} \end{bmatrix}, \tag{A.7}$$

$$[\mathbf{D}'(0,\rho,\omega)] = \begin{bmatrix} d'_{11} & 0 & 0 \\ 0 & d'_{22} & d'_{23} \\ 0 & d'_{32} & d'_{33} \end{bmatrix}, \tag{A.8}$$

with d_{11}, d_{22}, etc. being complex functions of ρ and ω.

Without loss of generality, the modes can be assumed to be plane waves propagating in the x direction, i.e., $\gamma = 0$ and $\rho = \beta$. From Eq. (A.7), the dispersion Eq. (A.3) gives

$$d_{11}(\beta,\omega) = 0 \tag{A.9}$$

or

$$d_{22}(\beta,\omega)d_{33}(\beta,\omega) - d_{23}(\beta,\omega)d_{32}(\beta,\omega) = 0. \tag{A.10}$$

For a given frequency f, Eq. (A.9) gives the wavenumbers β for SH modes and Eq. (A.10) gives those for P-SV modes.

Inserting Eqs. (A.4) and (A.5) into Eq. (A.1), the forced displacements can be worked out

$$\tilde{u}_{10} = [\,1 \quad 0\,]\begin{bmatrix} d_{22} & d_{23} \\ d_{32} & d_{33} \end{bmatrix}^{-1}\begin{bmatrix} d'_{22} & d'_{22} \\ d'_{32} & d'_{33} \end{bmatrix}\begin{Bmatrix} \tilde{p}_x \\ \tilde{p}_z \end{Bmatrix}, \tag{A.11}$$

$$\tilde{v}_{10} = d_{11}^{-1}d'_{11}\tilde{p}_y, \tag{A.12}$$

$$\tilde{w}_{10} = [\,0 \quad 1\,]\begin{bmatrix} d_{22} & d_{23} \\ d_{32} & d_{33} \end{bmatrix}^{-1}\begin{bmatrix} d'_{22} & d'_{22} \\ d'_{32} & d'_{33} \end{bmatrix}\begin{Bmatrix} \tilde{p}_x \\ \tilde{p}_z \end{Bmatrix}. \tag{A.13}$$

Eqs. (A.11) and (A.13) show that, for plane waves propagating in the x direction, then a vertical load and/or a longitudinal load on the ground surface only excite(s) P-SV modes which only contribute to the vertical and longitudinal displacements of the ground surface.

References

[1] A.M. Kaynia, C. Madshus, P. Zackrisson, Ground vibration from high-speed trains: prediction and countermeasure, *Journal of Geotechnical and Geoenvironmental Engineering* 126 (2000) 531–537.

[2] V.V. Krylov, Generation of ground vibrations by superfast trains, *Applied Acoustics* 44 (1995) 149–164.

[3] H. Takemiya, Simulation of track–ground vibrations due to high-speed trains, *Proceedings of the Eighth International Congress on Sound and Vibration*, Hong Kong, China, 2001, pp. 2875–2882.
[4] C.G. Lai, A. Callerio, E. Faccioli, A. Martino, Mathematical modelling of railway-induced ground vibrations, *Proceedings of the International Workshop Wave 2000*, Bochum, Germany, 2000, pp. 99–110.
[5] H. Grundmann, M. Lieb, E. Trommer, The response of a layered halfspace to traffic loads moving along its surface, *Archive of Applied Mechanics* 69 (1) (1999) 55–67.
[6] X. Sheng, C.J.C. Jones, M. Petyt, Ground vibration generated by a load moving along a railway track, *Journal of Sound and Vibration* 228 (1) (1999) 129–156.
[7] X. Sheng, C.J.C. Jones, D.J. Thompson, A theoretical model for ground vibration from trains generated by vertical track irregularities, *Journal of Sound and Vibration* 272 (3–5) (2004) 937–965, this issue.
[8] C. Madshus, A.M. Kaynia, High-speed railway lines on soft ground: dynamic behaviour at critical train speed, *Journal of Sound and Vibration* 231 (3) (2000) 689–701.
[9] C.J.C. Jones, X. Sheng, M. Petyt, Simulations of ground vibration from a moving harmonic load on a railway track, *Journal of Sound and Vibration* 231 (3) (2000) 739–751.
[10] A.T. Peplow, C.J.C. Jones, M. Petyt, Surface vibration propagation over a layered elastic half-space with an inclusion, *Applied Acoustics* 56 (1999) 283–296.
[11] D.V. Jones, The surface propagation of ground vibration, PhD Thesis, University of Southampton, 1987.
[12] X. Sheng, C.J.C. Jones, M. Petyt, The Fourier transformed stationary and moving dynamic flexibility matrices of a layered ground, Technical Memorandum 873, Institute of Sound and Vibration Research, University of Southampton, 1999.
[13] X. Sheng, C.J.C. Jones, M. Petyt, Ground vibration generated by a harmonic load acting on a railway track, *Journal of Sound and Vibration* 225 (1) (1999) 3–28.
[14] J. Oscarsson, T. Dahlberg, Dynamic train/track/ballast interaction—computer models and full-scale experiments, *Vehicle System Dynamics* 29 (1998) 73–84.
[15] J. Jonsson, Comments to "Ground Vibration Generated by a Harmonic Load Moving Along a Railway Track", *Journal of Sound and Vibration* 236 (2) (2000) 359–366.
[16] X. Sheng, C.J.C. Jones, D.J. Thompson, A comparison of a theoretical model for quasi-statically and dynamically induced environmental vibration from trains with measurements, *Journal of Sound and Vibration* 267(3) (2003) 621–635.